

1 **Estimation of temporal and spatial variations in**
2 **groundwater recharge in unconfined sand aquifers using**
3 **Scots pine inventories**

4

5 **P. Ala-aho¹, P.M. Rossi¹ and B. Kløve¹**

6

7 [1] Water Resources and Environmental Engineering Research Group, Faculty of Technology,
8 University of Oulu, P.O. Box 4300, 90014 University of Oulu, Finland

9 Correspondence to: P. Ala-aho (perti.ala-aho@oulu.fi)

10

11

12

13

14

15

16

17

18

19

20

21

22

23

24

25

26 **Abstract**

27 Climate change and land use are rapidly changing the amount and temporal distribution of
28 recharge in northern aquifers. This paper presents a novel method for distributing Monte Carlo
29 simulations of 1-D sandy sediment profile spatially to estimate transient recharge in an
30 unconfined esker aquifer. The modeling approach uses data-based estimates for the most
31 important parameters controlling the total amount (canopy cover) and timing (thickness of the
32 unsaturated zone) of groundwater recharge. Scots pine canopy was parameterized to leaf area
33 index (LAI) using forestry inventory data. Uncertainty in the parameters controlling sediment
34 hydraulic properties and evapotranspiration was carried over from the Monte Carlo runs to the
35 final recharge estimates. Different mechanisms for lake, soil, and snow evaporation and
36 transpiration were used in the model set-up. Finally, the model output was validated with
37 independent recharge estimates using the water table fluctuation method and baseflow
38 estimation. The results indicated that LAI is important in controlling total recharge amount.
39 Soil evaporation compensated for transpiration for areas with low LAI values, which may be
40 significant in optimal management of forestry and recharge. Different forest management
41 scenarios tested with the model showed differences in annual recharge of up to 100 mm. The
42 uncertainty in recharge estimates arising from the simulation parameters was lower than the
43 interannual variation caused by climate conditions. It proved important to take unsaturated
44 thickness and vegetation cover into account when estimating spatially and temporally
45 distributed recharge in sandy unconfined aquifers.

46

47

48

49

50

51

52

53

54

55 **1 Introduction**

56 Eskers are permeable, unconfined sand and gravel aquifers (Banerjee, 1975). In addition to
57 water supply, they support groundwater-dependent ecosystems and provide recreational
58 services (Kløve et al., 2011). Esker hydrology is important as eskers and other glaciofluvial
59 aquifer types cover large areas of the North and are among the dominant aquifer types in the
60 boreal zone. Management of these complex aquifers has gained recent attention (Bolduc et al.,
61 2005, Karjalainen et al., 2013, Koundouri et al., 2012, Kurki et al., 2013). The European
62 Groundwater Directive requires such systems to be characterized in order to determine their
63 quality status, so knowledge of how to estimate groundwater recharge in esker aquifers is
64 becoming increasingly important (EC, 2006). Esker aquifers are commonly covered with
65 managed pine forests, where the forest canopy is likely to influence recharge amounts. The soil
66 surface profile of eskers is complex and highly variable, consisting of kettle holes and sand
67 dunes, resulting in variable thickness of the unsaturated zone (Aartolahti, 1973), a factor which
68 also needs to be accounted for in recharge estimation.

69 Computational methods to estimate groundwater recharge vary from simple water balance
70 models, where water stores and fluxes are represented conceptually and related with adjustable
71 parameters (Jyrkama et al., 2002), to physically-based models using the Richards equation
72 (Assefa and Woodbury, 2013, Okkonen and Kløve, 2011) to solve water fluxes through
73 unsaturated zone. Computational methods solving the Richards equation are often limited to
74 small-scale areal simulations (Scanlon et al., 2002a) and shallow unsaturated zones, and they
75 commonly lack the soil freeze, thaw, and snow storage sub-routines relevant at higher northerly
76 latitudes (Okkonen, 2011). However, computational approaches can be employed to produce
77 the values on spatial and temporal variability in recharge often needed in groundwater modeling
78 (Dripps and Bradbury, 2010). The methods commonly rely on a GIS platform for spatial
79 representation and calculation approaches based on water balance to create the temporal
80 dimension of recharge (Croteau et al., 2010, Dripps and Bradbury, 2007, Jyrkama et al., 2002,
81 Sophocleous, 2000, Westenbroeck et al., 2010). Neglecting variations in thickness of the
82 unsaturated zone is common practice in many water balance models used in recharge
83 estimations. However, the residence time in the unsaturated zone may play an important role,
84 especially in the timing of recharge in deep unsaturated zones (Hunt et al., 2008), as
85 acknowledged in recent work (Assefa and Woodbury, 2013, Jyrkama and Sykes, 2007, Scibek
86 and Allen, 2006, Smerdon et al., 2008).

87 In numerical recharge models, actual evapotranspiration (ET) is a difficult variable to estimate
88 accurately from climate, soil, and land use data. The vegetation is commonly parameterized
89 from land use or land cover maps (Assefa and Woodbury, 2013, Jyrkama et al., 2002, Jyrkama
90 and Sykes, 2007, Keese et al., 2005), where the vegetation characteristics and leaf area index
91 (LAI) are estimated based solely on vegetation type. In addition to tree canopy transpiration,
92 soil evaporation, i.e. evaporation from the pores of soil matrix, can constitute a large proportion
93 of total ET. Soil evaporation from the forest floor is generally reported to range from 3 to 40%
94 of total ET (Kelliher et al., 1993), although values as high as 92% have been recorded (Kelliher
95 et al., 1998). For conifer forest canopies, soil evaporation can largely compensate for low
96 transpiration in areas with lower LAI (Ohta et al., 2001, Vesala et al., 2005). Data on canopy-
97 scale evaporation rates at latitudes above 60°N are rare (Kelliher et al., 1993). A few studies
98 have estimated ET from pine tree stands at patch scale (Kelliher et al., 1998, Lindroth, 1985),
99 but none has extended this analysis to spatially distributed groundwater recharge. Forest
100 management practices have the potential to affect the transpiration characteristics of coniferous
101 forests, which typically leads to increased groundwater recharge (Bent, 2001, Lagergren et al.,
102 2008, Rothacher, 1970).

103 The overall aim of the study was to provide novel information on groundwater recharge rates
104 and factors contributing to the amount, timing, and uncertainty of groundwater recharge in
105 unconfined sandy eskers aquifers. Study expands the application of physically-based 1-D
106 unsaturated water flow modeling for groundwater recharge, while taking into account detailed
107 information on vegetation (pine, lichen), unsaturated layer thickness, cold climate, and
108 simulation parameter uncertainty. Furthermore, this study considers the effect that forestry land
109 use has on vegetation parameters and how this is reflected in groundwater recharge.

110

111 **2 Materials and Methods**

112 **2.1 Study site**

113 Groundwater recharge was estimated for the case of the Rokua esker aquifer in northern Finland
114 (Fig. 1). Rokua is an unconfined aquifer consisting of unconsolidated sandy sediments
115 underlain by crystalline bedrock (Fig. 2). Aquifer was formed during previous deglaciation
116 when rivers under the melting ice sheet deposited sandy sediments in the river bed (Aartolahti
117 1973). The Rokua esker has a rolling surface topography in the aquifer recharge area rising

118 about 60 m above the flat peatland areas surrounding the esker. In the groundwater discharge
119 areas, the aquifer is locally confined by peat soil with low hydraulic conductivity (Rossi et al.
120 2012).

121 The climate at the Rokua aquifer is characterized by precipitation exceeding evapotranspiration
122 on an annual basis and statistics of the annual climate for the study period 1961 - 2010 in terms
123 of precipitation, air temperature and FAO reference evapotranspiration according to Allen et al.
124 (1998) is presented in Table 1. Another important feature of the climate is annually recurring
125 winter periods when most precipitation is accumulated as snow.

126 2.1.1 Leaf area index from forestry inventories

127 Forestry inventory data from the Finnish Forest Administration (Metsähallitus, MH) and
128 Finnish Forest Centre (Metsäkeskus, MK) were used to estimate LAI for the Rokua esker
129 groundwater recharge area. The available data consisted of 2786 individual plots covering an
130 area of 52.4 km² (62.4% of the model domain). The forestry inventories, performed mainly
131 during 2000-2011, showed that Scots pine (*Pinus sylvestris*) is the dominant tree in the model
132 area (94.2% of plots). The forest inventory data include a number of data attributes and the
133 following data fields, included in both the MH and MK datasets, were used in the analysis:

- 134 - Plot area (p_A); [ha]
- 135 - Main canopy type
- 136 - Average tree stand height (h); [m]
- 137 - Average stand diameter at breast height (d_{bh}); [cm]
- 138 - Number of stems (n_{stm}); [1 ha^{-1}]
- 139 - Stand base area (b_A); [$\text{m}^2 \text{ ha}^{-1}$]
- 140 - Stand total volume (V); [m^3]

141 Inventory plots were excluded from the analysis if: (1) main canopy type was not pine forest,
142 (2) data were missing for d_{bh} and h or n_{stm} , or (3) the MH and MK datasets overlapped, in which
143 case MH was retained. However, several plots in the MH dataset were lacking n_{stm} data, which
144 would have created a large gap in data coverage. Therefore the n_{stm} variable was estimated with
145 a log-transformed regression equation using data on d_{bh} , p_A , and V as independent variables.
146 This regression equation was built from 280 plots ($R^2 = 0.88$) and used to estimate n_{stm} for 288
147 plots. LAI was estimated as described by Koivusalo et al. (2008). Needle mass for an average

148 tree in stand/plot was estimated from h and d_{bh} using empirical equations presented by Repola
149 et al. (2007). LAI for a stand was calculated as:

$$150 \quad LAI = N_t * n_{stm} * S_{LA} \quad (1)$$

151 where N_t = needle mass per average tree in stand [kg], n_{stm} = number of stems per hectare
152 [1 ha^{-1}], and S_{LA} = specific leaf area = $4.43 \text{ m}^2 \text{ kg}^{-1} = 4.43 * 10^{-4} \text{ ha kg}^{-1}$ (Xiao et al., 2006).

153 Detailed information on LAI was used to obtain an estimate of how different forest management
154 options, already actively in operation in the area, could potentially affect groundwater recharge.
155 Three scenarios were simulated testing the potential impact of forestry operations on
156 groundwater recharge:

- 157 1) The first “baseline” scenario simulated the current situation by using LAI pattern at
158 the site (Fig. 3) estimated with Eq. (1).
- 159 2) The second scenario simulated the impact of intensive forestry operations as clear-
160 cutting of the tree stand. Clear-cutting is an intensive land use form where almost the
161 entire tree stand is removed, and it is carried out in some parts of the study area. Low
162 LAI values of 0-0.2 for the whole study site were used in simulating this scenario.
- 163 3) The third scenario simulated the impact of no forestry operations, i.e. absence of
164 forestry cuttings. The hypothetical mature stand covering the study site was assumed
165 to have high LAI values of 3.2-3.5 found at the study site and reported in the literature
166 (Koivusalo et al., 2008, Rautiainen et al., 2012, Vincke and Thiry, 2008, Wang et al.,
167 2004).

168 2.1.2 Lichen water retention

169 An organic lichen layer covers much of the sandy soil at the Rokua study site (Kumpula et al.,
170 2000), so this lichen layer was introduced in soil evaporation (SE) calculations. Although
171 lichens do not transpire water, their structural properties allow water storage in the lichen matrix
172 and capillary water uptake from the soil (Blum, 1973, Larson, 1979). In this study lichen layer
173 was explicitly included in the simulations to create an additional storage for water before the
174 mineral sandy sediments. Water interception storage by the lichen layer was estimated from
175 lichen samples. In total, six samples (species *Cladonia stellaris* and *C. rangiferina*) were taken
176 in May 2011 from two locations 500 m apart, close to borehole MEA506 (see Fig. 1). These
177 samples were collected by pressing plastic cylinders (diameter 10.6 cm) through the lichen layer
178 and extracting intact cores, after which mineral soil was carefully removed from the base of the

179 sample. Thus the final sample consisted of a lichen layer on top and a layer of organic litter and
180 decomposed lichen at the bottom, and was sealed in a plastic bag for transportation. To obtain
181 estimates of water retention capacity, the samples were first wetted until saturation with a
182 sprinkler, left overnight at +4 °C to allow gravitational drainage and weighed to determine ‘field
183 capacity’. The samples were then allowed to dry at room temperature and weighed daily until
184 stable final weight (‘dry weight’) was reached. The water retention capacity (w_r) of the sample
185 was calculated as:

$$186 \quad w_r = \frac{m_{fc} - m_{dry}}{\rho_w} \cdot \frac{1}{\pi \cdot r^2} \quad (2)$$

187 where m_{fc} is the field capacity weight [M], m_{dry} is the final dry weight [M] at room temperature,
188 ρ_w [M L⁻³] is the density of water, and r [L] is the radius of the sampling cylinder.

189 The mean water retention capacity of the lichen samples was found to be 9.85 mm (standard
190 deviation (SD) 2.71 mm) and approximations for these values were used in model
191 parameterization (Table 2). Measured lichen water retention capacity was introduced to the
192 simulations using parameters for soil porosity and layer thickness. Lichen porosity values were
193 varied between 7.5 - 12.5 % in simulation Monte Carlo runs (see section 2.2.1) while keeping
194 thickness of the lichen layer at 100 mm. In this manner the maximum amount of water retained
195 by the lichen layer after gravitational drainage was adjusted to vary between 7.5 mm - 12.5 mm,
196 as seen in the measurement data. To acknowledge the lack of information about B&C parameter
197 estimates for lichen, the parameters were included in the simulations Monte Carlo runs with
198 ranges which in our opinion produced reasonable shape of the pressure-saturation curve
199 allowing easy drainage of the lichen.

200 2.1.3 Sandy sediment hydraulic properties

201 Sediment texture was determined by sieving (ISO 3310-1 standard sieve, US sieve numbers 5,
202 10, 18, 35, 60, 120, and 230) 26 samples taken from five boreholes at various depths (Fig. 1).
203 14 of the samples were analyzed also for pressure saturation curves. Samples were characterized
204 as fine or medium sand, while sediment texture in the other boreholes (Fig. 1) had previously
205 been characterized as medium, fine or silty sand throughout the model domain by the Finnish
206 Environmental Administration as expert *in-situ* analysis during borehole drilling. Therefore the
207 sediment samples from the five boreholes were considered to be representative of the sediment
208 type in the area. Pressure saturation data from the samples was then used to define parameter
209 ranges for the Brooks and Corey equation used in the simulations (Table 2). Furthermore,

210 texture values were employed to calculate the range of saturated vertical hydraulic conductivity
211 for the samples, using empirical equations by Hazen, Kozeny-Carman, Breyer, Slitcher, and
212 Terzaghi (Odong, 2007). The hydraulic conductivity for a given sample ranged approximately
213 one order of magnitude between the equations. When using the five equations for the 26
214 samples in total, the calculated values were within $1.99 \cdot 10^{-5} - 1.47 \cdot 10^{-3} \text{ [m s}^{-1}\text{]}$ for all but one
215 sample. The obtained range was considered to reasonably represent the hydraulic conductivity
216 variability in the study area and simulations.

217 2.1.4 Climate data

218 Driving climate data for the model were taken from Finnish Meteorological Institute databases
219 for the modeling period 1 Jan 1961-31 Oct 2010. Daily mean temperature [$^{\circ}\text{C}$] and sum of
220 precipitation [mm] were recorded at Pelso climate station, 6 km south of the study area (Fig.
221 1). The most representative long-term global radiation data [$\text{kJ m}^{-2} \text{ d}^{-1}$] for the area were
222 available as interpolated values in a 10 x 10 km grid covering the whole of Finland. The
223 interpolation data point was found to be at approximately the same location as borehole
224 MEA2110 (Fig. 1). Long-term data on wind speed [m s^{-1}] and relative humidity [%] were taken
225 from Oulunsalo and Kajaani airports, located 60 and 40 km from the study site, respectively.
226 The data from the airports were instantaneous observations at three-hour intervals, from which
227 daily mean values were calculated. All the climate variables were recorded at reference height
228 2 m except for wind speed, which was measured at 10 m height. The wind speed data were
229 therefore recalculated to correspond to 2 m measurement height according Allen et al. (1998)
230 by multiplying daily average wind speed by 0.748. The suitability of long-term climate data for
231 the study site conditions was verified with observations made at a climate station established at
232 the study site in an overlapping time period (Dec 2009-Oct 2010) and the agreement between
233 the measurements was found to be satisfactory.

234 Data on long-term lake surface water temperature were needed to calculate lake evaporation
235 (see section 2.2.3), but were not available directly at the study site. However, surface water
236 temperature was recorded at Lake Oulujärvi by the Finnish environmental administration
237 (2013) 22 km from the study site in the direction of the Kajaani climate station (Fig. 1). The
238 Oulujärvi water temperature was found to be closely correlated (linear correlation coefficient
239 0.97) with daily lake water temperature recorded at Rokua during summer 2012. Daily lake
240 surface temperature data for Lake Oulujärvi starting from 21 July 1970 were used in lake
241 evaporation modeling. However, the data series had missing values for early spring and some

242 gaps during five years in the observation period. These missing values were estimated with a
243 sine function, corresponding to the average annual lake temperature cycle, and a daily time
244 series was established for subsequent calculations.

245 Snowmelt was calculated with a degree-day approach model in Jansson and Karlberg (2004).
246 Snow routines were calibrated separately using bi-weekly snow water equivalent (SWE) data
247 from Vaala snowline measurements (Finnish environment administration, 2011) for the period
248 1960-2010 (Fig. 1). This separately calibrated snow model was used for all subsequent
249 simulations.

250 **2.2 Recharge modeling framework**

251 **2.2.1 Water flow simulation in 1-D unsaturated sediment profile**

252 Water flow through an unsaturated one-dimensional (1-D) sandy sediment profile (Fig. 2) was
253 estimated with the Richards equation using CoupModel (Jansson and Karlberg, 2004).
254 CoupModel was selected as the simulation code because of its ability to represent the full soil-
255 plant-atmosphere continuum adequately and to include snow processes in the simulations
256 (Okkonen and Kløve, 2011). The simulated sediment profile was vertically discretized into 61
257 layers with increasing layer thickness deeper in the profile. Layer thickness was 0.1 m for the
258 first 16 layers (until 1.6 m), where the topmost 0.1 m was represented as a lichen layer. Layer
259 thickness was progressively increased by defining 0.2 m thickness for the next 7 layers
260 (between 1.6 and 3 m), 0.5 m for the next 14 layers (between 3 and 10 m), 1 m for the next 7
261 layers (between 10 and 17 m) and 2 m for last 17 layers ranging from 17 m to the bottom of the
262 profile (51 m).

263 The time variable boundary condition for water flow at the top of the column was defined by
264 driving climate variables and affected by sub-routines accounting for snow processes with daily
265 time step. The short time step was chosen to fully capture the main recharge input from
266 snowmelt. All water at the top of the domain was assumed to be subjected to infiltration. Deep
267 percolation as gravitational drainage was allowed from sediment column base using the unit-
268 gradient boundary condition (see e.g. Scanlon et al., 2002b). Simulations for the unsaturated 1-
269 D sediment profile were made for the period 1970-2010, and before each run 10 years of data
270 (1960-1970) were used to spin up the model.

271 The simulation of the 1-D sediment profile was performed 400 times as Monte Carlo runs to
272 facilitate the propagation of model parameter uncertainty in the final model output. Model was
273 ran each time with different parameter values as specified in Table 2. For each individual
274 simulation homogeneity in the vertical direction in terms of sediment hydraulic properties was
275 assumed. The parameters for which values were randomly varied were chosen beforehand by
276 trial and error model runs exploring the sensitivity of parameters with respect to cumulative
277 recharge or evapotranspiration. The parameter ranges were specified from field data when
278 possible; otherwise we resorted to literature estimates or in some cases used $\pm 50\%$ of the
279 CoupModel default providing a typical parameter for the used equation.

280 The sensitivity of the parameters varied in the simulations was tested with Kendall correlation
281 analysis, by testing the correlation between each model parameter and cumulative sums of
282 different evapotranspiration components and infiltration for the 400 model runs. Individual
283 simulation with unique parameter values did not produce a groundwater recharge value due to
284 the assembling strategy for recharge; therefore the ET components and infiltration were selected
285 as variables for comparison. In addition, correlations were examined as scatter plots to ensure
286 that possible sensitivity not captured by the monotonic correlation coefficient was not
287 overlooked.

288 2.2.2 Method to distribute 1-D simulations spatially

289 Groundwater recharge was estimated for a model domain of 82.3 km² (Fig. 1). To distribute the
290 simulations in 1-D sediment column spatially, the simulation domain was subdivided into
291 different recharge zones, similarly to e.g. Jyrkämä et al. (2002). Zonation in the model was
292 based on two variables: LAI and unsaturated zone thickness (UZT). The calculation of spatially
293 distributed values for LAI and UZT is presented in detail in sections 2.1.1 and 2.1.4. Both
294 variables were presented as a grid maps with 20m x 20m cell size with a floating point number
295 assigned to each cell, resulting in a total of 205 708 cells for the model domain. The small
296 model cell size was selected to ensure full exploitation of the forest inventory plots in LAI
297 determination. The spatially distributed data were then divided into 15 classes for LAI and 30
298 classes for UZT. The classes are primarily equal intervals, which was convenient in the
299 subsequent data processing, but in addition the frequency distributions of LAI and UZT cell
300 values were used to assign narrower classes for parameter ranges with many values (see
301 histograms in Figs. 3 and 4). Class interval for LAI was 0.2 units up to a value of 2 (class 1:
302 LAI = 0-0.2, etc.) and 0.3 to the maximum LAI value of 3.5. Class interval for UZT was 1 m

303 to 10 m depth and 2 m to the final depth of 51 m. Finally, the classified LAI and UZT data were
 304 combined to a raster map with 20m x 20m cell size, producing 449 different zones with unique
 305 combinations of LAI and UZT values. Spatial coupling was done with the ArcGIS software
 306 (ESRI, 2011).

307 Variation in the LAI and UZD parameters were used to allocate the 1-D sediment profile
 308 simulations spatially to the study site. LAI class in model cell specified a subset of the 400 1-
 309 D simulations that were applicable for a given cell. UZT class for each cell (Fig. 2) specified
 310 the depth in the simulated 51 m sediment profile where the water flux output was extracted.
 311 Using this approach each unique recharge zone (a combination of UZT and LAI class) had on
 312 average 27 water flow time series (number of total model runs [400] divided by number of LAI
 313 cell classes [15]) produced by different random combinations of parameters (Table 2). Equation
 314 (3) was used to propagate the variability in the 27 time series into the final areal recharge.

$$315 \quad R_{i,j} = \frac{\sum_{l=1}^{449} n(l) * R_{S_{i,rand(1:k)}} * A_c}{A_{tot}} \quad (3)$$

316 where $R_{i,j}$ is the final sample of areal recharge [mm day^{-1}], i is the index for simulation time
 317 step ($= 1:14975$), j is the index for sample for a given time step ($1:150$), l is the index for unique
 318 recharge zone, $n(l)$ is the number of cells in a given recharge zone, R_s is the recharge sample
 319 [mm/day] for a given recharge zone at time step I , k is the number of time series for a given
 320 recharge zone, A_c is the surface area of a model raster cell ($=20 \text{ m} * 20 \text{ m} = 400 \text{ m}^2$), and A_{tot}
 321 is the surface area of the total recharge area.

322 The resulting R matrix has 150 time series for areal recharge produced by simulations with
 323 different parameter realizations. The variability between the time series provides an indication
 324 of how much the simulated recharge varies due to different model parameter values. The
 325 method allows computationally efficient recharge simulations, because the different recharge
 326 zones do not all have to be simulated separately.

327 The simulation approach assumes that: (1) over the long-term, the water table remains at a
 328 constant level, i.e. the unsaturated thickness for each model cells stays the same. Monitoring
 329 data from 11 boreholes and seven lakes with more than 5 years of observation history shows
 330 level variability of 1 – 1.5 m, with depressions and recoveries of the water table. This variability
 331 is within the accuracy of water table estimation by interpolation. (2) the capillary fringe in the
 332 sandy sediment is thin enough not to affect the water flow before arriving at the ‘imaginary’
 333 water table at the center of each UZT class. (3) only vertical flow takes place in the unsaturated

334 sediment matrix, a typical assumption in recharge estimation techniques (Dripps and Bradbury,
335 2010, Jyrkama et al., 2002, Scanlon et al., 2002a). (4) surface runoff is negligible primarily due
336 to the permeable sediment type (as noted by Keese et al., 2005), and also due to lichen cover
337 inhibiting runoff by increasing surface roughness (Rodríguez-Caballero et al., 2012). The
338 maximum observed daily rainfall for the area has been 57.4 mm. Further assuming that rain for
339 the day fell only during one hour, it would equal to $1.59 \cdot 10^{-5} \text{ m s}^{-1}$ input rate of water, which
340 is close to the lower range of saturated hydraulic conductivity at the study site ($1.99 \cdot 10^{-5} \text{ m s}^{-1}$).
341 Therefore rainstorms at the site very rarely exceed the theoretical infiltration capacity. As a
342 field verification, surface runoff has not been observed during field visits and the area lacks
343 intermittent or ephemeral stream networks.

344 2.2.3 Estimation of evapotranspiration

345 Four different evaporation processes were considered in this study (Fig. 5); soil evaporation
346 (evaporation from the topmost soil layer, i.e. the lichen matrix), snow evaporation (evaporation
347 from snow surface), transpiration (evaporation through the vascular system of tree canopy) and
348 lake evaporation (evaporation from free water surface). The first three components were
349 estimated, along with water flow simulations, using CoupModel. However, as 3.6 % (2.9 km^2)
350 of the surface area of the study site consists of lakes (Fig. 1), lake evaporation from free water
351 surfaces was calculated independently from the CoupModel simulations.

352 Transpiration from the Scots pine canopy ($L_v E_{tp}$) was calculated using Penman-Monteith (P-
353 M) combination (Appendix 1, Eq. 1). Whenever possible, all the parameters relating to the P-
354 M equation were estimated based on data, namely LAI of the canopy. Surface resistance and
355 saturation vapor pressure difference are the main factors controlling conifer forest
356 evapotranspiration, while the aerodynamic resistance is of less importance (Lindroth, 1985,
357 Ohta et al., 2001). In the calculation of aerodynamic resistance with the P-M equation,
358 roughness length is related to LAI and canopy height, according to Shaw and Pereira (1982).
359 Other parameters governing the aerodynamic resistance, except for LAI, were treated as
360 constant. The surface resistance of the pine canopy was estimated with the Lohammar equation
361 (see e.g. Lindroth, 1985), accounting for effects of solar radiation and air moisture deficit in
362 tree canopy gas exchange. Because LAI values have a strong influence in the surface resistance
363 Lohammar equation, the other parameters governing the surface resistance were excluded from
364 the Monte Carlo runs. Distribution of root biomass with respect to depth from the soil surface
365 was presented with an exponential function, because most Scots pine roots are concentrated in

366 the shallow soil zone. A typical root depth value of 1 m was used for the entire canopy
367 (Kalliokoski, 2011, Kelliher et al., 1998, Vincke and Thiry, 2008). Soil and snow evaporation
368 were calculated using an empirical approach (Appendix 1, Eq. 4) based on the P-M equation,
369 as described in detail in Jansson and Karlberg (2004). Soil evaporation is calculated for the
370 snow-free fraction of the soil surface, and the snow evaporation is solved separately as a part
371 of snow pack water balance.

372 In areas where the water table is close to the ground surface, the water table can provide an
373 additional source of water for evapotranspiration (Smerdon et al., 2008). To take into account
374 the decreased recharge for areas with near surface water tables, the recharge for cells with an
375 unsaturated zone of <1 m (8.3% of the study site, 6.8 km²) was estimated with a water balance
376 approach. We assumed that for areas with a shallow water table, soil water content was not a
377 limiting factor for transpiration. Therefore an additional water source for transpiration was
378 considered by making the transpiration rate equal to simulated potential transpiration (T) during
379 times when the actual transpiration was simulated (T > 0.05 mm). Increasing effect of the water
380 table located at 1 m depth on soil evaporation was tested with simulations and found to be 5-
381 10% higher with than without a water table. Therefore a 7% addition was made to the simulated
382 actual soil evaporation for cells with a shallow water table. Daily recharge (R_{1m} , L T⁻¹) for cells
383 with unsaturated thickness below 1 m was estimated as:

$$384 \quad R_{1m} = I - T_{adj} - ES_{adj} \quad (4)$$

385 where I is infiltration water arriving to lake/soil surface, including both meltwater from the
386 snowpack and precipitation [L T⁻¹], T_{adj} [mm d⁻¹] is adjusted transpiration, and ES_{adj} [mm d⁻¹]
387 is adjusted soil evaporation. Kettle hole lakes in esker aquifers often lack surface water inlets
388 and outlets and are therefore an integral part of the groundwater system (Ala-aho et al., 2013,
389 Winter et al., 1998), so we considered these lakes as contributors to total groundwater recharge.
390 In other words, rainfall per lake surface area is treated equally as addition to the aquifer water
391 storage as groundwater recharge. As a difference, lake water table is subjected to evaporation
392 unlike the groundwater table. Lake evaporation (E_{lake}) was estimated with the mass transfer
393 approach (see e.g. Dingman, 2008) according to Eq. (7) in Appendix 1. The mass transfer
394 method was selected because of its simplicity, daily output resolution, low data requirement,
395 and physically-based approach. However various calculation methods could easily be used in
396 the modelling framework, depending on the data availability (see e.g. Rosenberry et al., 2007).
397 If lake percentage in the area of interest is high, more sophisticated methods may be required

398 to better represent the system. For the Rokua site the bias introduced by a simplistic approach
399 was considered minor.

400 **2.3 Model validation**

401 Model performance was tested by comparing the simulated recharge values with two
402 independent recharge estimates in local and regional scale; the water table fluctuation (WTF)
403 method and base flow estimation, respectively. The WTF method is routinely used to estimate
404 groundwater recharge because of its simplicity and ease of use. It assumes that any rise in water
405 level in an unconfined aquifer is caused by recharge arriving at the water table. For a detailed
406 description of the method and its limitations, see e.g. Healy and Cook (2002). The recharge
407 amount (R , $L T^{-1}$) is calculated based on the water level prior to and after the recharge event
408 and the specific yield of the sandy sediments:

$$409 \quad R = S_y \frac{\Delta h}{\Delta t} \quad (5)$$

410 where S_y is the specific yield, h is the water table height [L], and t is the time of water table rise
411 [T].

412 The WTF method requires groundwater level data with adequate resolution for both time and
413 water level, to identify periods of rising and falling water table. Water table was monitored
414 using pressure-based dataloggers (Solinst Levellogger Gold) recording with hourly interval
415 from six water table wells with average unsaturated zone thicknesses of 1.2, 1.6, 5.0, 8.0, 9.3,
416 and 14.7 m (Fig. 1). Wells where the water table was <2 m from the ground surface responded
417 to major precipitation events. In the deeper wells, only the recharge from snowmelt was seen
418 as water table rise. Estimates of the sandy sediment specific yield are required for the
419 calculations (Eq. 5), but no sediment samples were available from the wells used in water table
420 monitoring. Drilling records for these wells reported fine and medium sand, which was
421 consistent with the particle size distribution for other wells in the area. Therefore an estimated
422 value of 0.20-0.25 for the specific yield of all wells was used, according to typical values for
423 fine and medium sand (Johnson, 1967).

424 The recharge estimated with the WTF method was compared with the simulated recharge
425 during the recorded water level rise in the well. For each well, the cumulative sum of simulated
426 water flow was extracted from sediment profile depth corresponding to well water table depth.
427 As an example, the simulated recharge in well ROK1 (unsaturated thickness on average 14.7

428 m) was extracted from UTZ class 12, corresponding to recharge for unsaturated thickness of
429 14-16 m. All 400 model runs were used, providing 400 estimates for recharge for each time
430 period of recorded water level rise.

431 A regional estimate of groundwater recharge was estimated as baseflow of streams originating
432 at the groundwater discharge area. Because the Rokua esker aquifer acts as a regional water
433 divide, stream flow was monitored around the esker, in total of 18 locations (Fig. 1). The flows
434 were measured total of 8 times between 6 July 2009 and 3 August 2010 (see Rossi et al., 2014).
435 The lowest total outflow during 9-10 February 2010 was recorded after three months of snow
436 cover period, when water contribution to streams from surface runoff was minimal. The
437 minimum outflow was considered as baseflow from the aquifer reflecting long term
438 groundwater recharge in the area.

439

440 **3 Results**

441 **3.1 Model validation with the WTF and baseflow methods**

442 Model validation showed that the modeling approach could reasonably reproduce (1) the main
443 groundwater recharge events when compared to the WTF method (Fig. 6) and (2) the regional
444 level of recharge compared to stream baseflow. The WTF method agreed well with the
445 simulated values, with overlapping estimates between the methods for all but two recharge
446 events. Also the median value of simulations was close to WTF method, with some bias to
447 higher estimates from the simulations. The discrepancy can be due to very different assumptions
448 behind the methods and uncertainty in local parameterization; in the WTF method for the
449 specific yield (S_y) and for simulations mainly the hydraulic conductivity which dictates the
450 simulated timing of recharge. Uncertainty in the S_y estimate is acknowledged by showing S_y a
451 range rather than a single value (Fig. 6), but still S_y is not truly known for the location of
452 observation boreholes. Simplifying assumptions and subjective interpretation of both timing
453 and height of water table rise create additional inaccuracies in the WTF estimate.

454 Independent regional estimate of recharge, stream baseflow, was $70\ 500\ \text{m}^3\ \text{s}^{-1}$, or $312.7\ \text{mm}$
455 a^{-1} when related to the recharge area. The order of magnitude agreed with long term simulated
456 average of $362.8\ \text{mm}\ \text{a}^{-1}$. Typical error in individual stream flow measurements is within 3-6 %
457 of the measured value (Sauer and Meyer, 1992), which brings minor uncertainty in the baseflow
458 value. The smaller value for stream baseflow compared to simulated long term average recharge

459 can be explained with conceptual understanding of site hydrogeology (Ala-aho et al., 2015,
460 Ala-aho et al., 2013, Rossi et al., 2012, Rossi et al., 2014). Part of the recharged groundwater
461 does not discharge to the small streams whose baseflow was measured, but flows underneath
462 the stream catchments and seeps out to regional surface bodies (Lake Oulujärvi and River
463 Oulujoki) further away from the recharge area (Fig. 2). Fully integrated surface-subsurface
464 hydrological modeling study of the same site presented in Ala-aho et al. (2015) simulated an
465 outflow of 79 mm a⁻¹ to regional surface water bodies.

466 **3.2 Temporal variations in groundwater recharge**

467 When recharge simulation time series were summarized to annual values (1 Oct-30 Sept),
468 recharge rates co-varied with annual infiltration with linear correlation coefficient of 0.89
469 (Fig. 7) as expected based on previous work in humid climate and sandy aquifers (Keese et al.,
470 2005, Lemmelä, 1990). Both annual recharge and infiltration displayed an increasing trend. The
471 plot also showed the level of uncertainty in annual recharge values introduced by differences
472 in model parameterization (black area). The difference between minimum and maximum value
473 for simulated annual recharge was on average 23.0 mm. Thus the variability in recharge
474 estimates was 6.3 % of mean annual recharge 362.8 mm.

475 According to the simulations, the *effective rainfall*, i.e. the percentage of corrected rainfall
476 resulting in groundwater recharge annually, was on average 59.3%. This is in agreement with
477 previous studies on unconfined esker aquifers at northerly latitudes, in which the proportion of
478 annual precipitation percolating to recharge is reported to be 50-70% (71% by Zaitsoff (1984),
479 54% by Lemmelä and Tattari (1986) and 56% by Lemmelä (1990)). The percentage of effective
480 rainfall varied considerably, by almost 30 %-units, between different hydrological years, from
481 44.8% in some years up to 73.1% in others.

482 **3.3 Influence of LAI on spatial variation of groundwater recharge**

483 The spatial distribution of groundwater recharge was mostly due to variations in LAI, but also
484 influenced by distance to water table, and distribution of lakes (Fig. 8). Higher evaporation rates
485 from lakes led to lower recharge in lakes (see red spots in Fig. 8). Similarly, high LAI led to
486 high ET and resulted in low recharge in plots with high LAI. Other areas of low recharge,
487 although not as obvious at the larger spatial scales shown in Fig. 8, were cells with a shallow

488 water table (section 2.2.2). The effect of high ET at locations with a shallow water table can
489 best be seen in south-east parts of the aquifer.

490 Kendall correlation analysis of simulation parameters and annual average model outputs
491 identified LAI as the most important parameter controlling evapotranspiration and infiltration
492 (Table 3). Parameters related to sediment hydraulics and evaporation showed some sensitivity
493 to simulation results, while the parameters for lichen vegetation were only slightly sensitive or
494 insensitive to simulation output variables. The LAI parameter governed the level of evaporation
495 for different ET components (Fig. 9). Evaporation from soil (and snow) compensated for mean
496 annual ET for LAI values up to around 1.0, after which total ET increased as a function of LAI.

497 The scenarios for low (0 ... 0.2) and high (3.2 ... 3.5) LAI changed the groundwater recharge
498 rates compared to the current LAI distribution (in Fig. 7). In the high LAI scenario the annual
499 recharge was on average 101.7 mm lower than in the low LAI scenario. These results suggest
500 that management of the Scots pine canopy has a significant control on the total recharge rates
501 in unconfined esker aquifers.

502 Average land surface ET components remained relatively constant between years, but the
503 simulated ET displayed a wide spread between simulations (Fig. 10). Estimated annual
504 evapotranspiration (mean 237.6 mm) was somewhat lower than previous regional estimates of
505 total ET (300 mm; (Mustonen, 1986)). Lake evaporation rates were generally higher than
506 evapotranspiration from the land surface (420.0 mm). The variation in simulated lake
507 evaporation was considerably lower than that in ET, as a different approach was used to account
508 for uncertainty in the simulations. Transpiration showed greater variation between simulations
509 than soil evaporation and total land surface ET. On average, transpiration also comprised a
510 slightly larger share of total evaporation than soil evaporation. Simulated snow evaporation was
511 a small, yet not insignificant, component in the total ET.

512 **4 Discussion**

513 The method used here to estimate LAI from forestry inventories introduces a new approach for
514 incorporating large spatial coverage of detailed conifer canopy data into groundwater recharge
515 estimations. LAI values reported for conifer forests in Nordic conditions similar to the study
516 site are in the range 1-3, depending on canopy density and other attributes (Koivusalo et al.,
517 2008, Rautiainen et al., 2012, Vincke and Thiry, 2008, Wang et al., 2004). The LAI values
518 obtained for the study site (mean 1.25) were at the lower end of this range. Furthermore, the
519 data showed a bimodal distribution, with many model cells with low LAI (< 0.4) lowering the

520 mean LAI. The low LAI values were expected because of active logging and clearcutting
521 activities in the study area. Although the equations to estimate LAI are empirical in nature and
522 based on simplified assumptions, the method can outline spatial differences in canopy structure.
523 Wider use of this method in Finland is practically possible, as active forestry operations in
524 Finland have yielded an extensive database on canopy coverage, which could be used in
525 groundwater management. However, the LAI estimation method could be further validated with
526 field measurements or Lidar techniques (Chasmer et al., 2012, Riaño et al., 2004).

527 Plant cover, represented as LAI, proved to be the most important model parameter important
528 parameter controlling total ET, and thereby the amount of groundwater recharge (Table 3, Fig.
529 9). The LAI parameter was included in the equations controlling both transpiration and soil
530 evaporation, and therefore the sensitivity of the parameter is not surprising. While soil
531 evaporation partly compensated for the lower transpiration with low LAI values, the total
532 annual ET values progressively increased as a function of LAI (Fig. 9). Interestingly, the
533 simulations suggested that ET remains constant at constant level in the LAI range 0-1,
534 potentially due to the sparse canopy changing the aerodynamic resistance and partitioning of
535 radiation limiting soil evaporation, while still not contributing much to transpiration in total ET.
536 This implies that the maximum groundwater recharge for boreal Scots pine remains rather
537 constant up to a threshold LAI value of around 1. This knowledge can be used when co-
538 managing forest and groundwater resources in order to optimize both.

539 Importance of LAI has been reported in earlier studies estimating groundwater recharge
540 (Dripps, 2012, Keese et al., 2005, Sophocleous, 2000), but here the vegetation was represented
541 with more spatially detailed patterns and a field data-based approach for LAI. According to
542 previous studies, average ET from boreal conifer forests is around 2 mm d^{-1} during the growing
543 season (Kelliher et al., 1998), which is similar to our average value of 1.6 mm d^{-1} for the period
544 1 May-31 Oct. Some earlier studies have claimed that the influence of LAI on total ET rates
545 from boreal conifer canopies is minor (Kelliher et al., 1993, Ohta et al., 2001, Vesala et al.,
546 2005), but our simulation results indicate that higher LAI values lead to higher total ET values.
547 The simulations showed that variable intensity of forestry, from low canopy coverage (LAI =
548 0-0.2) to dense coverage (LAI = 3.2-3.5) resulted in a difference of over 100 mm in annual
549 recharge (Fig. 7). It can be argued that the scenarios are unrealistic, because high LAI values,
550 covering the whole study site, may not be achieved even with a complete absence of forestry
551 operations. Nevertheless, the result demonstrates a substantial impact of forestry operations on

552 esker aquifer groundwater resources. The lichen layer covering the soil surface was explicitly
553 accounted for in the simulation set-up, which to our knowledge is a novel modification. Kelliher
554 et al. (1998) concluded that precipitation intercepted by lichen was an important source of
555 understorey evaporation, especially directly after rain events. In addition, Bello and Arama
556 (1989) reported that lichen could intercept light rain showers completely and that only intense
557 rain events caused drainage from lichen canopy to mineral soil. While the lichen layer might
558 have an increasing effect on soil evaporation through ‘interception storage’, Fitzjarrald and
559 Moore (1992) suggest that a lichen cover may in fact have an insulating influence on heat and
560 vapor exchange between soil and atmosphere, therefore impeding evaporation from the mineral
561 soil. In the present study, the lichen layer appeared to have minor influence on total evaporation,
562 soil evaporation and infiltration, as these variables showed only little sensitivity to lichen B&C
563 parameters (Table 3). However, the approach to represent lichen with B&C model needs to
564 better examined, as water retention capacity of lichen layer was introduced to the simulations
565 using the concept of total porosity, which is not strictly coherent with the B&C model.
566 Nevertheless, the used approach successfully produced an additional dynamic interception
567 storage of water in the correct range (generally 3-7 mm depending on random parameterization,
568 data not shown). The performed laboratory measurement of lichen water retention should be
569 supplemented with detailed analysis of lichen pressure-saturation curve and hydraulic
570 conductivity to clarify the role of lichen in soil evaporation, and thereby groundwater recharge.

571 Stochastic variation of selected model parameters illustrated the uncertainties relating to
572 numerical recharge estimation using the Richards equation in one dimension. The capability
573 and robustness of the Richards equation to reproduce soil water content and water fluxes have
574 been demonstrated extensively in various studies (Assefa and Woodbury, 2013, Scanlon et al.,
575 2002b, Stähli et al., 1999, Wierenga et al., 1991). Therefore we considered that model
576 calibration and validation with point observations of variables such as soil volumetric water
577 content or soil temperature would not provide novel insights into water flow in unsaturated
578 porous media. Instead, we incorporated the parameter uncertainty ranges, usually used in model
579 calibration, to the final recharge simulation output. An important outcome was that the
580 uncertainty in the model output caused by different model parameterizations was small in
581 comparison with the interannual variation in recharge. The error caused by uncertainty in the
582 model assumptions or driving climate data was not addressed in this study.

583 The sensitivity analysis focused on total cumulative values of fluxes and did not address the
584 temporal variations in the variables. Sediment hydraulic parameters mainly influenced the
585 timing of recharge through residence time in the unsaturated zone, not so much the total amount.
586 Therefore the sediment hydraulic parameters showed only minor sensitivity, perhaps
587 misleadingly. It should be noted that vertical heterogeneity in the unsaturated sediment profile
588 hydraulic parameters can reduce the total recharge rates (Keese et al., 2005). However, vertical
589 heterogeneities were ignored in this study not only to simplify the model, but also because the
590 drilling logs showed only little variation in the area. Work of Wierenga et al. (1991) supports
591 the simplification by showing that excluding moderate vertical heterogeneities does not
592 significantly affect the performance of water flow simulations with the Richards equation.

593 Simulations acknowledged shallow water table contribution to evapotranspiration in an
594 indirect, conceptual approach. Including a water table fixed at different depths in the sediment
595 profile would have been possible in the CoupModel setup. Influence of water table fixed at 2
596 m depth was tested and found to increase ET 3.5% for LAI values of 3, but for LAI values of
597 0.5 and 1.5 the increase in ET was only trivial. We expect only minor increase in ET with deeper
598 water table configuration (with the given sediment texture), and therefore argue that excluding
599 water table results in only minimal overestimation of total recharge at the study site. It should
600 be noted that upward water fluxes were not excluded from the water flow time series and
601 negative fluxes were considered as “negative recharge” at any depth. The simplification is made
602 that water available for upward fluxes comes only from the soil moisture storage, not from the
603 water table.

604 According to the simulations, the percentage of precipitation forming groundwater recharge
605 varied considerably between years, as also reported in previous studies on transient recharge
606 (Assefa and Woodbury, 2013, Dripps and Bradbury, 2010). Even though annual recharge was
607 correlated with annual precipitation, and therefore years with high precipitation resulted in
608 higher absolute recharge (Fig. 7), the percentage of effective rainfall did not increase as a
609 function of annual sum of precipitation. This is somewhat surprising, because the rather
610 constant evaporation potential between years (Fig. 10) and high sediment hydraulic
611 conductivity could be expected to result in a higher percentage of rainfall reaching the water
612 table in rainy years. Some studies (Dripps and Bradbury, 2010, Okkonen and Kløve, 2010) have
613 suggested that when the main annual water input arrives as snowmelt during the low
614 evaporation season, it is likely to result in higher percentage recharge than in a year with little

615 snow storage and precipitation distributed evenly throughout summer and autumn, which may
616 contribute to the variability in the effective rainfall coefficient. However, when the maximum
617 annual SWE value was used as a proxy for annual snow storage, there was no evidence of snow
618 amount explaining the interannual variability in the recharge coefficient. Other factors
619 contributing to recharge coefficient variability may be related to soil moisture conditions prior
620 to snowfall, or the intensity of summer precipitation events (Smerdon et al., 2008, Stähli et al.,
621 1999).

622 The above-mentioned reasons make the concept of effective rainfall, which is currently
623 routinely used to estimate groundwater recharge for groundwater management in e.g. Finland
624 (Britschgi et al., 2009), susceptible to over- or under-estimation of actual annual recharge. This
625 applies especially for aquifers with a thick unsaturated zone, where rainy years produce higher
626 average recharge with some delay and for a longer duration (Zhou, 2009).

627

628 **5 Conclusions**

629 A physically-based approach to simulate groundwater recharge for sandy unconfined aquifers
630 in cold climates was developed. The method accounts for the influence of vegetation,
631 unsaturated zone thickness, presence of lakes, and uncertainty in simulation parameters in the
632 recharge estimate. It is capable of producing spatially and temporally distributed groundwater
633 recharge values with uncertainty margins, which are generally lacking in recharge estimates,
634 despite understanding of uncertainty related to recharge estimates being potentially crucial for
635 groundwater resource management. However, the parameter uncertainty defined for the study
636 area was of minor significance compared with interannual variations in the recharge rates
637 introduced by climate variations.

638 The simulations showed that Scots pine canopy, parameterized as leaf area index (LAI), was
639 important in controlling the total amount of groundwater recharge. Forestry inventory databases
640 were used to estimate and spatially allocate the LAI and the results showed that such inventories
641 could be better utilized in groundwater resource management. Forest cuttings were
642 demonstrated to increase groundwater recharge significantly. A sensitivity analysis on the
643 parameters used showed that soil evaporation could compensate for low LAI-related
644 transpiration up to a LAI value of approximately 1, which may be important in finding the
645 optimal level for forest management in groundwater resource areas. The concept of effective
646 rainfall gave inconsistent estimates of recharge in annual timescales, showing the importance

647 of using physically-based recharge estimation methods for sustainable groundwater recharge
648 management.

649

650

651

652

653 **Author contribution**

654 P. Ala-aho and P.M Rossi collected and analyzed the field data. P. Ala-aho designed the
655 simulation set-up, performed the simulations and interpreted the results. P. Ala-aho prepared
656 the manuscript with contributions from all co-authors.

657

658 **Acknowledgements**

659 This study was made possible by the funding from EU 7th Framework programme GENESIS
660 (Contract Number 226536), Academy of Finland AKVA research program, the Renlund
661 Foundation, VALUE doctoral school and Maa- ja vesitekniikantuki ry. We would like to
662 express our gratitude to Geological survey of Finland, Finnish Forest Administration
663 (Metsähallitus) and Finnish Forest Centre (Metsäkeskus), Finnish meteorological institute,
664 Finnish environmental administration and National land survey of Finland for providing
665 datasets and expert knowledge that made this study possible in its current extent. To reproduce
666 the research in the paper, data from above mentioned agencies can be made available for
667 purchase on request from the corresponding agency, other data can be provided by the
668 corresponding author upon request. We thank Per-Erik Jansson for his assistance with the
669 CoupModel and Jarkko Okkonen (GTK), anonymous reviewer, and Angelo Basile for their
670 critical comments that significantly improved the manuscript.

671

672

673

674

675

676 **References**

- 677 Aartolahti, T.: Morphology, vegetation and development of Rokuanvaara, an esker and dune
678 complex in Finland, *Societas geographica Fenniae*, Helsinki, 1973.
- 679 Ala-aho, P., Rossi, P. M. and Kløve, B.: Interaction of esker groundwater with headwater
680 lakes and streams, *J. Hydrol.*, 500, 144-156, doi:10.1016/j.jhydrol.2013.07.014, 2013.
- 681 Ala-aho, P., Rossi, P. M., Isokangas, E. and Kløve, B.: Fully integrated surface–subsurface
682 flow modelling of groundwater–lake interaction in an esker aquifer: Model verification with
683 stable isotopes and airborne thermal imaging, *J. Hydrol.*, 522, 391-406,
684 doi:10.1016/j.jhydrol.2014.12.054, 2015.
- 685 Allen, R., Pereira, L., Raes, D. and Smith, M.: Crop evapotranspiration - Guidelines for
686 computing crop water requirements, Food and Agriculture Organization of the United
687 Nations, Rome, 1998.
- 688 Assefa, K. A. and Woodbury, A. D.: Transient, spatially- varied groundwater recharge
689 modelling, *Water Resour. Res.*, 49, 1-14, doi:10.1002/wrcr.20332, 2013.
- 690 Banerjee, I., McDonald, B.C.: Nature of esker sedimentation, in: *Glaciofluvial and*
691 *Glaciolacustrine Sedimentation*, edited by: Jopling, A. V. and McDonald, B. C., *Soc. Econ.*
692 *Paleontol. Mineral.*, Tulsa, U.S.A, 132-155, 1975
- 693 Bello, R. and Arama, A.: Rainfall interception in lichen canopies, *Climatol. Bull*, 23, 74-78,
694 1989.
- 695 Bent, G. C.: Effects of forest-management activities on runoff components and ground-water
696 recharge to Quabbin Reservoir, central Massachusetts, *For. Ecol. Manage.*, 143, 115-129,
697 2001.
- 698 Blum, O. B.: Water relations, in: *The lichens*, Ahmadjian, V. and Hale, M. E. (Eds.),
699 Academic Press Inc., USA, 381-397, 1973.
- 700 Bolduc, A., Paradis, S. J., Riverin, M., Lefebvre, R. and Michaud, Y.: A 3D esker geomodel
701 for groundwater research: the case of the Saint-Mathieu–Berry esker, Abitibi, Quebec,
702 Canada, in: *Three-Dimensional Geologic Mapping for Groundwater Applications: workshop*
703 *extended abstracts*, 17-20, Salt Lake City, Utah, 15 Oct, 2005.
- 704 Britschgi, R., Antikainen, M., Ekholm-Peltonen, M., Hyvärinen, V., Nylander, E., Siiro, P.
705 and Suomela, T.: Mapping and classification of groundwater areas, *The Finnish Environment*
706 *Institute*, Sastamala, Finland, 75 pp., 2009.
- 707 Chasmer, L., Pertrone, R., Brown, S., Hopkinson, C., Mendoza, C., Diiwu, J., Quinton, W.
708 and Devito, K.: Sensitivity of modelled evapotranspiration to canopy characteristics within
709 the Western Boreal Plain, Alberta, in: *Remote Sensing and Hydrology, Proceedings of a*
710 *Symposium at Jackson Hole*, 337-341, Wyoming, USA, 27-30 September 2010, 2012.

- 711 Croteau, A., Nastev, M. and Lefebvre, R.: Groundwater recharge assessment in the
712 Chateauguay River watershed, *Canadian Water Resources Journal*, 35, 451-468, 2010.
- 713 Dingman, S. L.: *Physical hydrology*, Waveland Press Inc, Long Grove, IL, 2008.
- 714 Dripps, W.: *An Integrated Field Assessment of Groundwater Recharge*, *Open Hydrology*
715 *Journal*, 6, 15-22, 2012.
- 716 Dripps, W. and Bradbury, K.: The spatial and temporal variability of groundwater recharge in
717 a forested basin in northern Wisconsin, *Hydrol. Process.*, 24, 383-392, doi:10.1002/hyp.7497,
718 2010.
- 719 Dripps, W. and Bradbury, K.: A simple daily soil–water balance model for estimating the
720 spatial and temporal distribution of groundwater recharge in temperate humid areas,
721 *Hydrogeol. J.*, 15, 433-444, doi:10.1007/s10040-007-0160-6, 2007.
- 722 EC: Directive 2006/118/EC of the European Parliament and of the Council on the protection
723 of groundwater against pollution and deterioration, Bryssels, Belgium, 2006.
- 724 ESRI: *ArcGIS Desktop: Release 10*, Environmental Systems research institute, Redlands,
725 Texas, 2011.
- 726 Finnish environmental administration: Oiva – the environmental and geographical
727 information service, Helsinki, Finland, Observation station number 5903320, Data extracted
728 27 June 2013, 2013.
- 729 Finnish environmental administration: Oiva – the environmental and geographical
730 information service, Helsinki, Finland, Observation station number 1592101, Data extracted
731 11 Feb 2011, 2011.
- 732 Fitzjarrald, D. R. and Moore, K. E.: Turbulent transports over tundra, *J. Geophys. Res.*, 97,
733 16717-16729, 1992.
- 734 Healy, R. W. and Cook, P. G.: Using groundwater levels to estimate recharge, *Hydrogeol. J.*,
735 10, 91-109, 2002.
- 736 Hunt, R. J., Prudic, D. E., Walker, J. F. and Anderson, M. P.: Importance of unsaturated zone
737 flow for simulating recharge in a humid climate, *Ground Water*, 46, 551-560, 2008.
- 738 Jansson, P. and Karlberg, L.: *Coupled heat and mass transfer model for soil-plant-atmosphere*
739 *systems*, Royal Institute of Technology, Dept of Civil and Environmental Engineering,
740 Stockholm, 435 pp., 2004.
- 741 Johnson, A. I.: *Specific yield: compilation of specific yields for various materials*, US
742 Government Printing Office, Washington, 1967.
- 743 Jyrkama, M. I. and Sykes, J. F.: The impact of climate change on spatially varying
744 groundwater recharge in the grand river watershed (Ontario), *J. Hydrol.*, 338, 237-250, 2007.

- 745 Jyrkama, M. I., Sykes, J. F. and Normani, S. D.: Recharge estimation for transient ground
746 water modeling, *Ground Water*, 40, 638-648, 2002.
- 747 Kalliokoski, T.: Root system traits of Norway spruce, Scots pine, and silver birch in mixed
748 boreal forests: an analysis of root architecture, morphology, and anatomy, Ph.D. thesis,
749 Department of Forest Sciences, Faculty of Agriculture and Forestry, University of Helsinki,
750 2011.
- 751 Karjalainen, T., Rossi, P., Ala-aho, P., Eskelinen, R., Reinikainen, K., Kløve, B., Pulido-
752 Velazquez, M. and Yang, H.: A decision analysis framework for stakeholder involvement and
753 learning in groundwater management, *Hydrol. Earth Syst. Sci.* 17, 5141-5153,
754 doi:10.5194/hess-17-1-2013, 2013.
- 755 Keese, K. E., Scanlon, B. R. and Reedy, R. C.: Assessing controls on diffuse groundwater
756 recharge using unsaturated flow modeling, *Water Resour. Res.*, 41, W06010,
757 doi:10.1029/2004WR003841, 2005.
- 758 Kelliher, F. M., Leuning, R. and Schulze, E. D.: Evaporation and canopy characteristics of
759 coniferous forests and grasslands, *Oecologia*, 95, 153-163, 1993.
- 760 Kelliher, F. M., Lloyd, J., Arneth, A., Byers, J. N., McSeveny, T. M., Milukova, I., Grigoriev,
761 S., Panfyorov, M., Sogatchev, A., Varlargin, A., Ziegler, W., Bauer, G. and Schulze, E. -:
762 Evaporation from a central Siberian pine forest, *J. Hydrol.*, 205, 279-296,
763 doi:10.1016/S0022-1694(98)00082-1, 1998.
- 764 Kløve, B., Ala-aho, P., Bertrand, G., Boukalova, Z., Ertürk, A., Goldscheider, N., Ilmonen, J.,
765 Karakaya, N., Kupfersberger, H., Kværner, J., Lundberg, A., Mileusnić, M., Moszczynska,
766 A., Muotka, T., Preda, E., Rossi, P., Siergieiev, D., Šimek, J., Wachniew, P., Angheluta, V.
767 and Widerlund, A.: Groundwater dependent ecosystems. Part I: Hydroecological status and
768 trends, *Environ. Sci. & Policy*, 14, 770-781, doi:10.1016/j.envsci.2011.04.002, 2011.
- 769 Koivusalo, H., Ahti, E., Laurén, A., Kokkonen, T., Karvonen, T., Nevalainen, R. and Finér,
770 L.: Impacts of ditch cleaning on hydrological processes in a drained peatland forest,
771 *Hydrol. Earth Syst. Sci.*, 12, 1211-1227, 2008.
- 772 Koundouri, P., Kougea, E., Stithou, M., Ala-Aho, P., Eskelinen, R., Karjalainen, T. P., Klove,
773 B., Pulido-Velazquez, M., Reinikainen, K. and Rossi, P. M.: The value of scientific
774 information on climate change: a choice experiment on Rokua esker, Finland, *Journal of*
775 *Environmental Economics and Policy*, 1, 85-102, 2012.
- 776 Kumpula, J., Colpaert, A. and Nieminen, M.: Condition, potential recovery rate, and
777 productivity of lichen (*Cladonia* spp.) ranges in the Finnish reindeer management area, *Arctic*,
778 53, 152-160, 2000.
- 779 Kurki, V., Lipponen, A. and Katko, T.: Managed aquifer recharge in community water
780 supply: the Finnish experience and some international comparisons, *Water Int.*, 38, 774-789,
781 2013.

- 782 Lagergren, F., Lankreijer, H., Kučera, J., Cienciala, E., Mölder, M. and Lindroth, A.:
783 Thinning effects on pine-spruce forest transpiration in central Sweden, *For. Ecol. Manage.*,
784 255, 2312-2323, 2008.
- 785 Larson, D. W.: Lichen water relations under drying conditions, *New Phytol.*, 82, 713-731,
786 doi:10.1111/j.1469-8137.1979.tb01666.x, 1979.
- 787 Lemmelä, R. and Tattari, S.: Infiltration and variation of soil moisture in a sandy aquifer,
788 *Geophysica*, 22, 59-70, 1986.
- 789 Lemmelä, R.: Water balance of sandy aquifer at Hyrylä in southern Finland, Ph.D. thesis,
790 University of Turku, Turku, 1990.
- 791 Lindroth, A.: Canopy Conductance of Coniferous Forests Related to Climate, *Water Resour.*
792 *Res.*, 21, 297-304, doi:10.1029/WR021i003p00297, 1985.
- 793 Mustonen, S.: *Sovellettu hydrologia, Vesiyhdistys*, Helsinki, 1986.
- 794 National Land Survey of Finland: NLS file service of open data, Laser scanning point cloud
795 (LiDAR), 2012.
- 796 Odong, J.: Evaluation of empirical formulae for determination of hydraulic conductivity
797 based on grain-size analysis, *Journal of American Science*, 3, 54-60, 2007.
- 798 Ohta, T., Hiyama, T., Tanaka, H., Kuwada, T., Maximov, T. C., Ohata, T. and Fukushima, Y.:
799 Seasonal variation in the energy and water exchanges above and below a larch forest in
800 eastern Siberia, *Hydrol. Process.*, 15, 1459-1476, doi:10.1002/hyp.219, 2001.
- 801 Okkonen, J.: Groundwater and its response to climate variability and change in cold snow
802 dominated regions in Finland: methods and estimations, Ph.D. thesis, University of Oulu,
803 Oulu, Finland, 78 pp., 2011.
- 804 Okkonen, J. and Kløve, B.: A conceptual and statistical approach for the analysis of climate
805 impact on ground water table fluctuation patterns in cold conditions, *J. Hydrol.*, 388, 1-12,
806 doi:10.1016/j.jhydrol.2010.02.015, 2010.
- 807 Okkonen, J. and Kløve, B.: A sequential modelling approach to assess groundwater–surface
808 water resources in a snow dominated region of Finland, *Journal of Hydrology*, 411, 91-107,
809 doi:10.1016/j.jhydrol.2011.09.038, 2011.
- 810 Rautiainen, M., Heiskanen, J. and Korhonen, L.: Seasonal changes in canopy leaf area index
811 and moDis vegetation products for a boreal forest site in central Finland, *Boreal*
812 *Environ. Res.*, 17, 72-84, 2012.
- 813 Repola, J., Ojansuu, R. and Kukkola, M.: Biomass functions for Scots pine, Norway spruce
814 and birch in Finland, Finnish Forest Research Institute (METLA), Helsinki, 28 pp., 2007.

- 815 Riaño, D., Valladares, F., Condés, S. and Chuvieco, E.: Estimation of leaf area index and
816 covered ground from airborne laser scanner (Lidar) in two contrasting forests, *Agric. For.*
817 *Meteorol.*, 124, 269-275, 2004.
- 818 Rodríguez-Caballero, E., Cantón, Y., Chamizo, S., Afana, A. and Solé-Benet, A.: Effects of
819 biological soil crusts on surface roughness and implications for runoff and erosion,
820 *Geomorphology*, 145, 81-89, 2012.
- 821 Rosenberry, D. O., Winter, T. C., Buso, D. C. and Likens, G. E.: Comparison of 15
822 evaporation methods applied to a small mountain lake in the northeastern USA, *Journal of*
823 *Hydrology*, 340, 149-166, 2007.
- 824 Rossi, P. M., Ala-aho, P., Ronkanen, A. and Kløve, B.: Groundwater - surface water
825 interacion between an esker aquifer and a drained fen, *J. Hydrol*, 432-433, 52-60,
826 doi:10.1016/j.jhydrol.2012.02.026, 2012.
- 827 Rossi, P. M., Ala-aho, P., Doherty, J. and Kløve, B.: Impact of peatland drainage and
828 restoration on esker groundwater resources: modeling future scenarios for management,
829 *Hydrogeol. J.*, doi:10.1007/s10040-014-1127-z, 2014.
- 830 Rothacher, J.: Increases in water yield following clear-cut logging in the Pacific Northwest,
831 *Water Resour. Res.*, 6, 653-658, 1970.
- 832 Sauer, V. B. and Meyer, R.W.:Determination of error in individual discharge measurements.
833 Open-File Report 92-144. U.S. Geological Survey, Norcross, Georgia, 1992.
- 834 Scanlon, B. R., Healy, R. and Cook, P.: Choosing appropriate techniques for quantifying
835 groundwater recharge, *Hydrogeol. J.*, 10, 91-109, 2002.
- 836 Scanlon, B. R., Christman, M., Reedy, R. C., Porro, I., Simunek, J. and Flerchinger, G. N.:
837 Intercode comparisons for simulating water balance of surficial sediments in semiarid regions,
838 *Water Resour. Res.*, 38, 59-1-59-16, doi:10.1029/2001WR001233, 2002.
- 839 Scibek, J. and Allen, D.: Modeled impacts of predicted climate change on recharge and
840 groundwater levels, *Water Resour. Res.*, 42, W11405, doi:10.1029/2005WR004742, 2006.
- 841 Shaw, R. H. and Pereira, A. R.: Aerodynamic roughness of a plant canopy: A numerical
842 experiment, *Agricultural Meteorology*, 26, 51-65, doi:10.1016/0002-1571(82)90057-7, 1982.
- 843 Smerdon, B., Mendoza, C. and Devito, K.: Influence of subhumid climate and water table
844 depth on groundwater recharge in shallow outwash aquifers, *Water Resour. Res.*, 44,
845 W08427, doi:10.1029/2007WR005950, 2008.
- 846 Sophocleous, M.: Quantification and regionalization of ground-water recharge in south-
847 central Kansas: integrating field characterization, statistical analysis, and GIS, *Spec Issue,*
848 *Compass*, 75, 101-115, 2000.
- 849 Stähli, M., Jansson, P. and Lundin, L. C.: Soil moisture redistribution and infiltration in
850 frozen sandy soils, *Water Resour. Res.*, 35, 95-103, 1999.

851 Vesala, T., Suni, T., Rannik, Ü, Keronen, P., Markkanen, T., Sevanto, S., Grönholm, T.,
852 Smolander, S., Kulmala, M. and Ilvesniemi, H.: Effect of thinning on surface fluxes in a
853 boreal forest, *Global Biogeochem. Cycles*, 19, GB2001, doi:10.1029/2004GB002316, 2005.

854 Vincke, C. and Thiry, Y.: Water table is a relevant source for water uptake by a Scots pine
855 (*Pinus sylvestris* L.) stand: Evidences from continuous evapotranspiration and water table
856 monitoring, *Agric. For. Meteorol.*, 148, 1419-1432, doi:10.1016/j.agrformet.2008.04.009,
857 2008.

858 Wang, Y., Woodcock, C. E., Buermann, W., Stenberg, P., Voipio, P., Smolander, H., Häme,
859 T., Tian, Y., Hu, J., Knyazikhin, Y. and Myneni, R. B.: Evaluation of the MODIS LAI
860 algorithm at a coniferous forest site in Finland, *Remote Sens. Environ.*, 91, 114-127,
861 doi:10.1016/j.rse.2004.02.007, 2004.

862 Westenbroeck, S. M., Kelson, V. A., Hunt, R. J. and Branbury, K.,R.: A modified
863 Thornthwaite-Mather Soil-Water-Balance code for estimating groundwater recharge, USGS,
864 Reston, Virginia, USA, 2010.

865 Wierenga, P., Hills, R. and Hudson, D.: The Las Cruces Trench Site: Characterization,
866 Experimental Results, and One-Dimensional Flow Predictions, *Water Resour. Res.*, 27, 2695-
867 2705, 1991.

868 Winter, T. C., Harvey, J. W., Franke, O. L. and Alley, W. M.: Ground water and surface
869 water; a single resource, USGS, Denver, Colorado, 79 pp., 1998.

870 Xiao, C., Janssens, I. A., Yuste, J. and Ceulemans, R.: Variation of specific leaf area and
871 upscaling to leaf area index in mature Scots pine, *Trees*, 20, 304-310, doi:10.1007/s00468-
872 005-0039-x, 2006.

873 Zaitsoff, O.: Groundwater balance in the Oripää esker, National Board of Waters, Finland,
874 Helsinki, 54-73 pp., 1984.

875 Zhou, Y.: A critical review of groundwater budget myth, safe yield and sustainability,
876 *J. Hydrol.*, 370, 207-213, doi:10.1016/j.jhydrol.2009.03.009, 2009.

877

878

879

880

881

882

883

884

885 **Tables**

886 **Table 1.** Characteristics of the study site annual climate.

VARIABLE	MEAN	STD
Precipitation [mm]	591	91
Air Temperature [°C]	-0.7	1.1
Reference ET [mm]	426	26

887

888 **Table 2.** Randomly varied parameters, related equations and parameter ranges included in the
889 model runs. For full description of parameters and equations, see Jansson and Karlberg (2004).

Parameter	Part of the model affected	Range	Units	Source
LAI (leaf area index)	Transpiration	0 ... 3.5	-	Data, see section 2.1.1
h (canopy height)	Transpiration	5 ... 15	m	Data
r_{lai} (increase in aerodynamic resistance with LAI)	Soil evaporation	25 ... 75	-	$\pm 50\%$, estimate
r_{ψ} (soil surface resistance control)	Soil evaporation	100...300	-	$\pm 50\%$ approximately to cover the surface resistance reported 150-1000 (Kelliher et al., 1998)
λ_L (pore size distribution index)	Soil evaporation, lichen	0.4 ... 1	-	Estimate, to cover an easily drainable range of pressure-saturation curves
Ψ_L (air entry)	Soil evaporation, lichen	1.5 ... 20	-	Estimate, to cover a easily drainable range of pressure-saturation curves
θ_L (porosity)	Soil evaporation, lichen	7.5...12.5	%	Data, lichen mean water retention $\pm SD$ from samples

$k_{mat,L}$ (matrix saturated hydraulic conductivity)	Soil evaporation, lichen	$5 \cdot 10^4 \dots 5 \cdot 10^7$	mm d ⁻¹	Estimate, high K values assumed
t_{WD} (coefficient in the soil temperature response function)	Water uptake	10 ... 20	-	±50%, estimate
Ψ_c (critical pressure head for water uptake reduction)	Water uptake	200...600	-	±50%, estimate
$k_{mat,S}$ (matrix saturated hydraulic conductivity)	Sediment profile	$1.707 \cdot 10^3 \dots 127.2 \cdot 10^3$	mm d ⁻¹	Data from sediment sample particle size analysis
k_{minuc} (minimum unsaturated hydraulic conductivity)	Sediment profile	$1 \cdot 10^{-4} \dots 1 \cdot 10^{-1}$	mm d ⁻¹	Estimate $k_{mat} \cdot 1E-5$
λ_s (pore size distribution index)	Sediment profile	0.4 ... 1	-	Range to cover measured pressure-saturation curves
Ψ_s (air entry)	Sediment profile	20 ... 40	-	Range to cover measured pressure-saturation curves
θ_s (porosity)	Sediment profile	0.25...0.36	%	Range from soil samples
θ_r (residual water content)	Sediment profile	0.01...0.05	%	Range to cover measured pressure-saturation curves

890

891

892

893

894

895

896

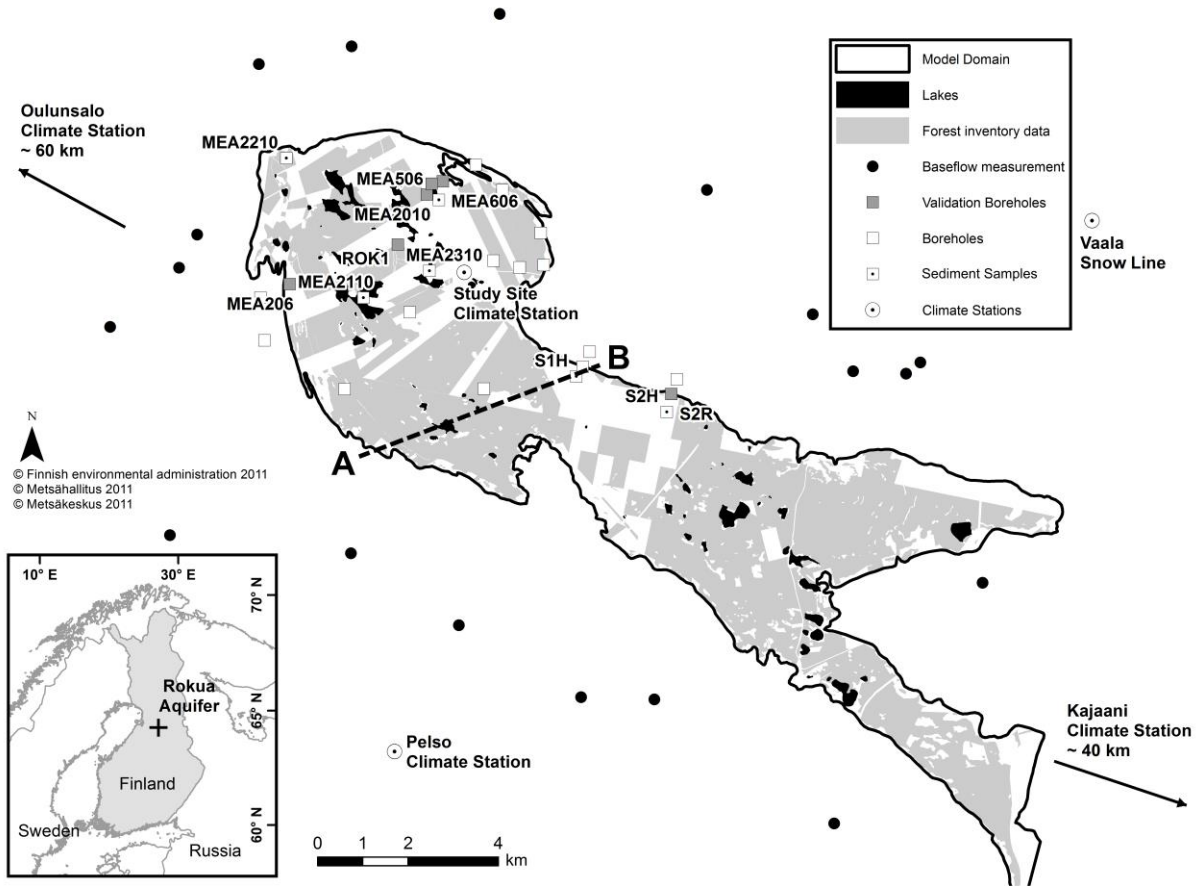
897

898 **Table 3.** Kendall correlation coefficient for simulation parameters and average annual sum of
 899 simulation output variables. ET = evapotranspiration, E = evaporation, for other symbols see
 900 Table 2.

Parameter	Total ET	Transpiration	Soil E	Snow E	Infiltration
LAI	0.59*	0.84*	-0.73*	-0.37*	0.18*
h	0.59*	0.84*	-0.73*	-0.37*	0.18*
r_{Ψ}	-0.11*	-0.03	-0.03	-0.61*	0.58*
r_{lai}	-0.13*	-0.02	-0.11*	0.03	-0.05
λ_L	-0.09*	-0.01	-0.11*	0.01	-0.03
Ψ_L	0.01	-0.04	0.11*	-0.04	0.06
θ_L	0.06	0.03	0.01	-0.00	0.09*
$k_{mat,L}$	-0.01	0.02	-0.04	-0.00	-0.00
$k_{mat,S}$	-0.10*	-0.04	-0.07*	0.02	0.01
k_{minuc}	-0.10*	-0.04	-0.07*	0.02	0.01
tWD	-0.05	-0.02	-0.03	-0.05	0.03
Ψ_c	0.18*	0.12*	-0.02	-0.04	0.05
λ_s	0.13*	0.06	0.06	-0.00	-0.23*
Ψ_s	-0.11*	-0.05	-0.04	-0.05	0.04
θ_s	0.02	-0.01	0.03	0.10*	-0.18*
θ_r	0.07*	0.05	-0.01	0.01	0.16*

901 *Significant correlation, $p < 0.05$

902

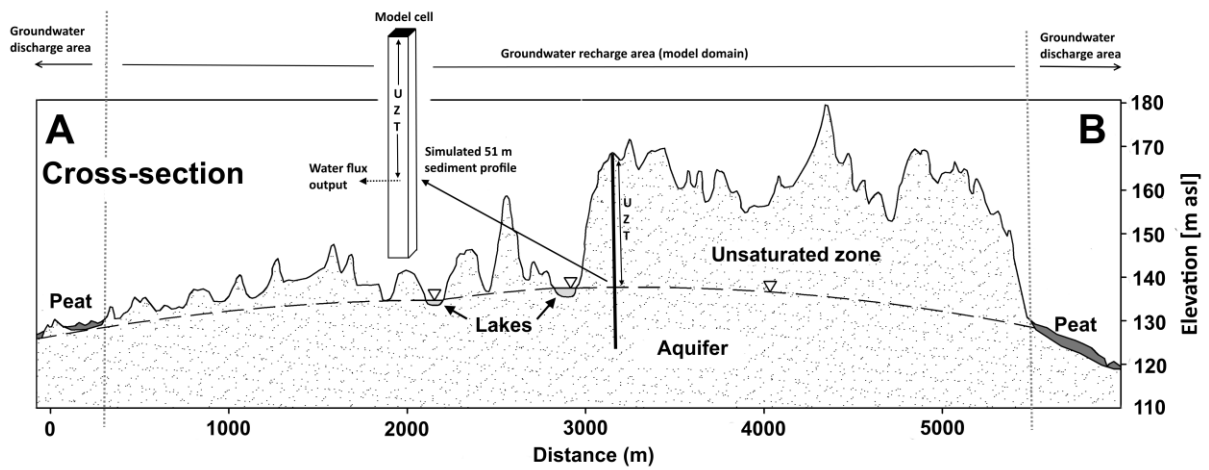


904
 905 **Figure 1.** Recharge area of the Rokua esker aquifer. Boreholes in the area were used for model
 906 validation and sediment type characterization. Baseflow was measured from streams
 907 originating outside the groundwater recharge area. Profile of cross-section A-B is presented in
 908 Fig. 2.

909

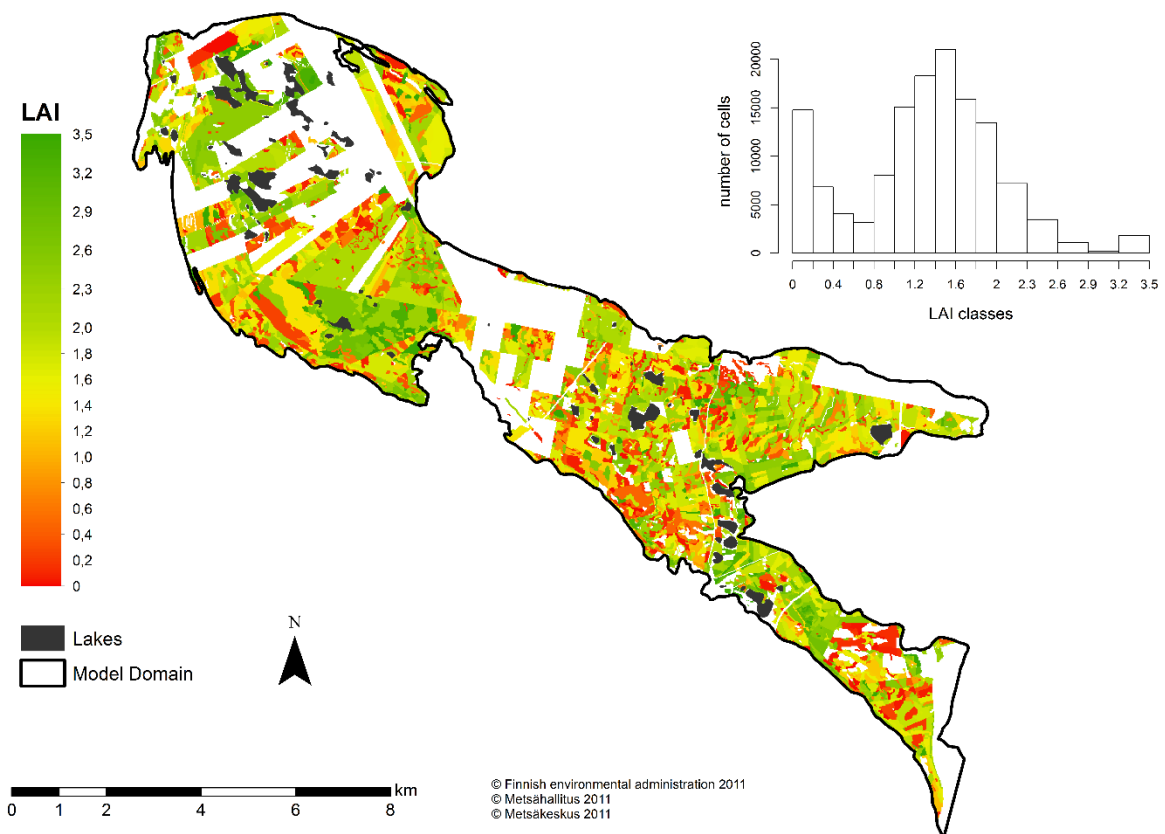
910

911



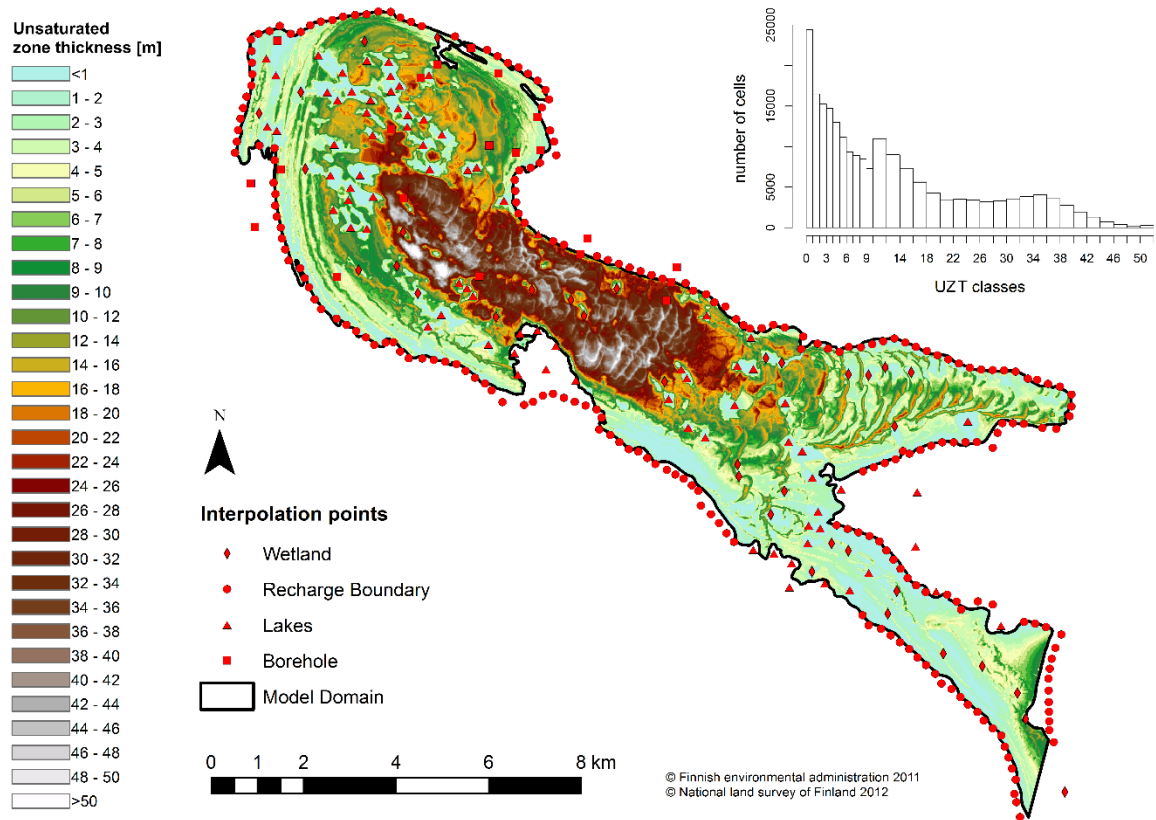
912

913 **Figure 2.** Cross-section A-B (Fig. 1) to demonstrate the geometry of the unsaturated zone and
 914 the aquifer (vertical axes exaggerated). A simulated sediment profile is shown to give an
 915 example on how 1-D simulations are represented in the model domain, UZT represents the
 916 unsaturated zone thickness parameter.



917

918 **Figure 3.** Spatial distribution of leaf area index (LAI) and a 20m x 20m cell-based histogram
 919 of LAI values. In areas where forestry inventory data were lacking, a weighted average value
 920 of 1.25 was used in simulations.

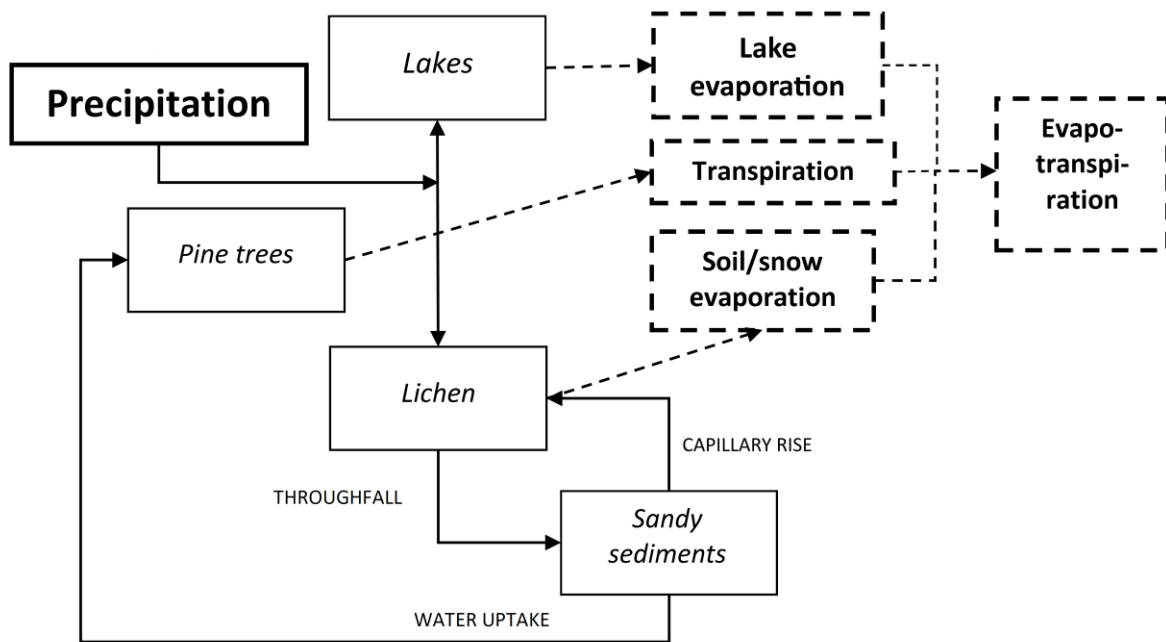


921

922 **Figure 4.** Estimated thickness of the unsaturated zone in the model area and interpolation points
 923 for estimation of water table elevation.

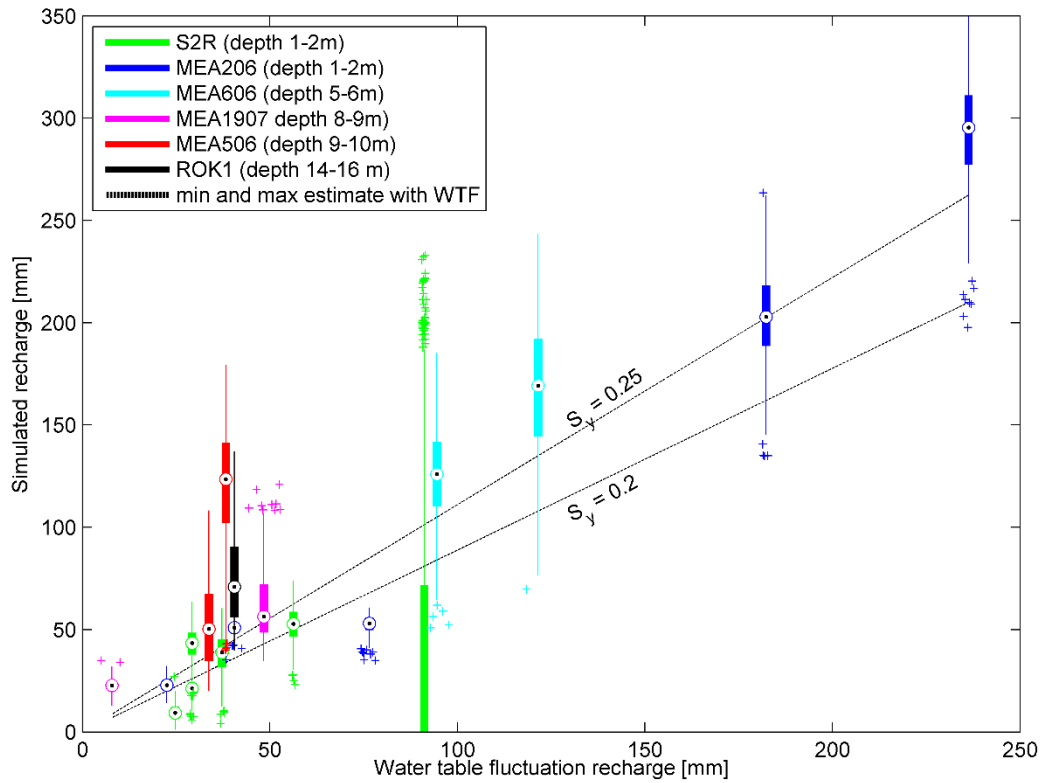
924

925



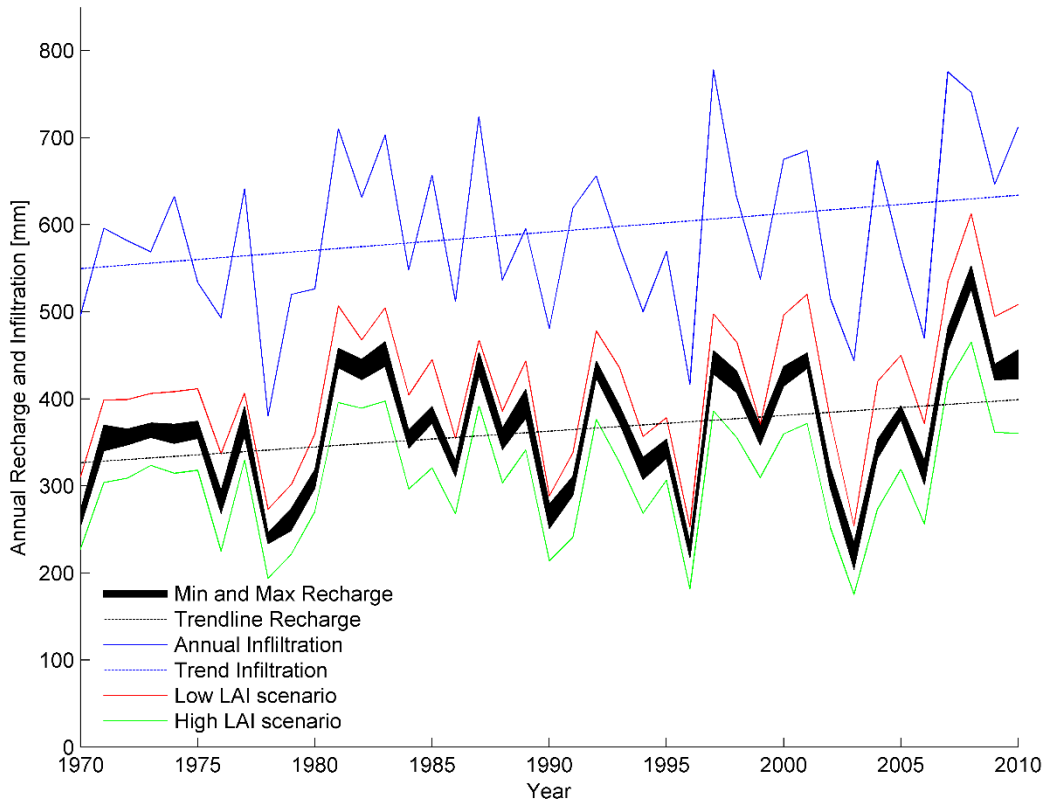
926

927 **Figure 5.** Flow chart of different evaporation processes considered in the study. Total
 928 evapotranspiration comprises of soil evaporation from the topmost soil layer, i.e. the lichen
 929 matrix, snow evaporation from snow surface, transpiration through the vascular system of tree
 930 canopy and lake evaporation from free water surface.



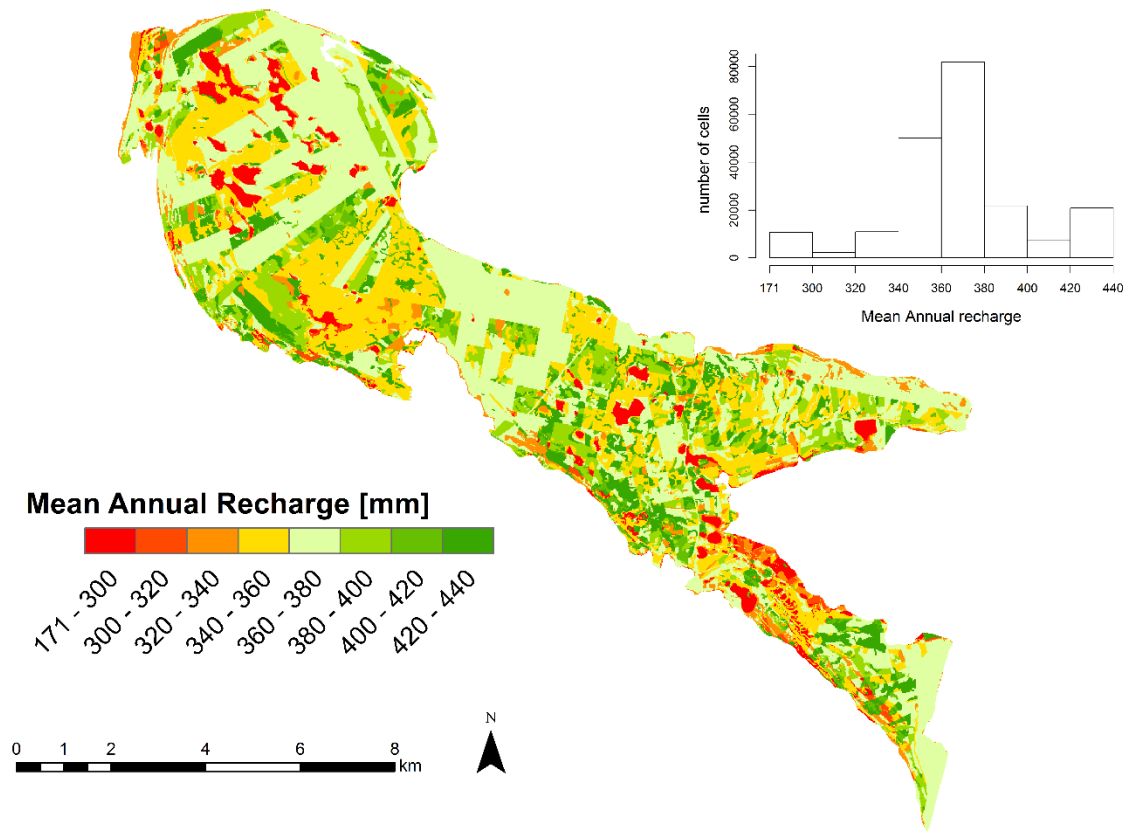
931

932 **Figure 6.** Assemblage of simulated recharge for individual recharge events, shown as boxplots
 933 where circles represent the median, bold lines 25-75th percentiles of the simulations, thin lines
 934 the remaining upper and lower 25th percentiles and crosses are outliers. The location of the
 935 boxplots on the x-axis is the WTF estimate for a given recharge event using a specific yield
 936 value of 0.225. The dashed lines indicate the uncertainty in the WTF estimates caused by the
 937 selection of specific yield. The two estimates would agree perfectly (given the uncertainty in
 938 S_y) if all simulations shown as boxplots fell between the dashed lines.



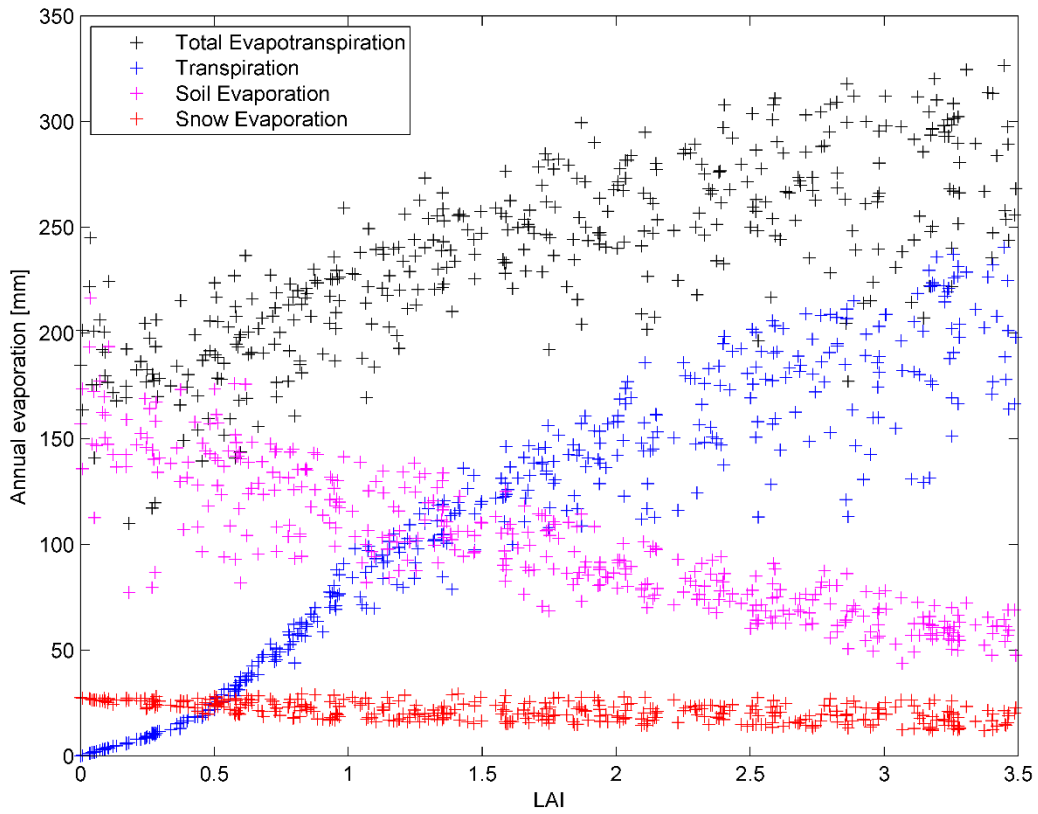
939

940 **Figure 7.** Annual recharge time series from simulations where the black area covers the
 941 minimum and maximum values for different recharge samples. The annual recharge pattern
 942 closely followed trends in infiltration. Effects of different land use management practices over
 943 time on annual recharge rates are shown as high and low leaf area index (LAI) scenarios.



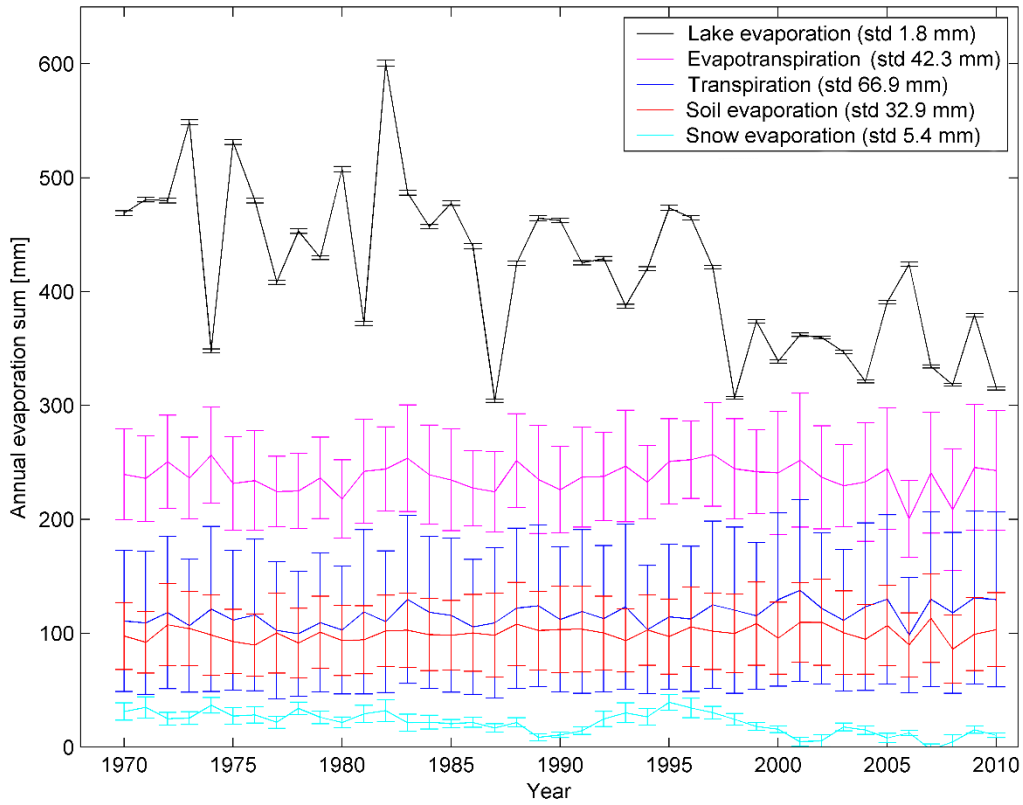
944

945 **Figure 8.** Spatial distribution of mean annual recharge, which was influenced mainly by the
 946 Scots pine canopy (LAI), the presence of lakes and, to some extent, areas with a shallow water
 947 table.



948

949 **Figure 9.** Example of scatter plots with the mean annual ET components are plotted as a
 950 function of the variable leaf area index (LAI), showing clear dependence of all ET components
 951 on LAI.



952

953 **Figure 10.** Values of different evapotranspiration (ET) components (mean and standard
 954 deviation) simulated for the study period.